

Charged and Pseudoscalar Higgs production at a Muon Collider

A.G. Akeroyd^a, A. Arhrib^{b,c} and C. Dove

*a: KEK Theory Group, Tsukuba,
Ibaraki 305-0801, Japan*

*b: Département de Mathématiques, Faculté des Sciences et Techniques
B.P 416, Tanger, Morocco*

*c: UFR-High Energy Physics, Physics Departement, Faculty of Sciences
PO Box 1014, Rabat, Morocco*

Abstract

We consider single charged Higgs (H^\pm) and pseudoscalar Higgs (A^0) production in association with a gauge boson at $\mu^+\mu^-$ colliders. We find that the tree-level t-channel and s-channel contributions to $\mu^+\mu^- \rightarrow H^\pm W^\mp, A^0 Z$ are enhanced for large values of $\tan\beta$, allowing sizeable cross-sections whose analogies at e^+e^- colliders would be very small. These processes provide attractive new ways of producing such particles at $\mu^+\mu^-$ colliders and are superior to the conventional methods in regions of parameter space.

1 Introduction

Charged Higgs bosons (H^\pm) are predicted in many favourable extensions of the Standard Model (SM), in particular the Minimal Supersymmetric Standard Model (MSSM). Their phenomenology [1] has received much attention both at e^+e^- colliders [2] and at hadron colliders [3], [4]. It is well known that e^+e^- colliders offer a much cleaner environment in which to look than hadron colliders, although recently progress has been made in the possibilities of detecting H^\pm for $M_{H^\pm} \geq m_t$ at hadron colliders [5]. At e^+e^- colliders production proceeds via the mechanism $e^+e^- \rightarrow \gamma^*, Z^* \rightarrow H^+H^-$, with higher order corrections evaluated in [6], and detection is possible for M_{H^\pm} up to approximately $\sqrt{s}/2$. The combined null-searches from all four LEP collaborations derive the lower limit $M_{H^\pm} \geq 77.3$ GeV (95% *c.l.*) [7].

In recent years an increasing amount of work has been dedicated to the physics possibilities of $\mu^+\mu^-$ colliders [8], [9]. Such colliders offer novel ways of producing Higgs bosons, such as an s -channel resonance in the case of neutral scalars. The existing studies do not highlight any difference between the charged Higgs phenomenology at a $\mu^+\mu^-$ collider and e^+e^- collider, and state that the main production mechanism would be via $\mu^+\mu^- \rightarrow \gamma^*, Z^* \rightarrow H^+H^-$. The rate for this process is identical at both colliders. In the MSSM H^\pm becomes roughly degenerate in mass with H^0 and A^0 for masses greater than 200 GeV. It is this correlation among the masses of the Higgs bosons which disallows any large effects from a s -channel resonance (via $\mu^+\mu^- \rightarrow H^0, h^0 \rightarrow H^+H^-$) in the pair production mode, and we explicitly confirm this. In order for the above to be maximised one would require $\sqrt{s} \approx M_{h,H} \geq 2M_{H^\pm}$, a condition which requires sizeable mass splittings among the Higgs bosons and is disallowed in the MSSM.

So far unconsidered is the process $\mu^+\mu^- \rightarrow H^\pm W^\mp$ via s -channel and t -channel diagrams. Naïvely, this may offer greater possibilities of a large rate since the Yukawa coupling only appears at one vertex in contrast to both vertices in the pair production case. In addition, it offers the possibility of searching for M_{H^\pm} up to $\sqrt{s} - M_W$ in contrast to pair production which only probes up to $M_{H^\pm} \leq \sqrt{s}/2$. The rate for $b\bar{b} \rightarrow H^\pm W^\mp$ at hadron colliders was considered in Ref. [10] although is not expected to provide an observable signature above the background [11], at least at LHC energies. In contrast, $\mu^+\mu^- \rightarrow H^\pm W^\mp$ might give a clean signature, since backgrounds are considerably less.

In an analogous way we also consider $\mu^+\mu^- \rightarrow A^0 Z$. The phenomenology of A^0 is made tricky at e^+e^- colliders due to the absence of a tree-level vertex ZZA^0 and so the standard Higgsstrahlung mechanism ($e^+e^- \rightarrow A^0 Z$) only proceeds via loops [12]. Moreover, over a wide region of parameter space in the MSSM A^0 has a suppressed rate in the channel $\mu^+\mu^- \rightarrow A^0 h^0$, while $\mu^+\mu^- \rightarrow A^0 H^0$ only probes up to $M_A \approx \sqrt{s}/2$. Proposed search strategies at $\mu^+\mu^-$ collider include the scanning technique and Bremsstrahlung tail method. Since both may provide a challenge for machine and detector design we consider the prospects of searching for A^0 via $\mu^+\mu^- \rightarrow A^0 Z$.

Our work is organized as follows. In Section 2 we perform the full tree-level calculation of $\mu^+\mu^- \rightarrow H^+H^-$, $\mu^+\mu^- \rightarrow H^\pm W^\mp$ and $\mu^+\mu^- \rightarrow A^0 Z$. In Section 3 we present numerical values of the cross-sections and Section 4 contains our conclusions.

2 Calculation

We now consider in turn the various production mechanisms. Our calculations are valid in both the MSSM and a general Two–Higgs–Doublet–Model (2HDM), the difference being that the MSSM Higgs sector is parametrized by just two parameters at tree–level (usually taken as M_A and $\tan\beta$), while the 2HDM contains 7 free parameters. Thus in a general 2HDM all four Higgs boson masses may be taken as independent, as well as the two mixing angles α and β , and the Higgs potential parameter λ_5 (in the notation of Ref. [13]). In addition, the Higgs trilinear couplings differ from those in the MSSM. In this paper we shall present numerical results for the MSSM. Let us summarise the couplings needed for our study:

Fermion–Fermion–Higgs couplings

$$\begin{aligned} h^0\mu^+\mu^- &= -\frac{igm_\mu}{2M_W}\lambda_{h\mu^+\mu^-} \quad , \quad H^0\mu^+\mu^- = -\frac{igm_\mu}{2M_W}\lambda_{H\mu^+\mu^-} \\ A^0\mu^+\mu^- &= -\frac{igm_\mu}{2M_W}\gamma_5\lambda_{A^0\mu^+\mu^-} \quad , \quad H^-\mu^+\nu_\mu = \frac{igm_\mu}{\sqrt{2}M_W}\lambda_{H^-\mu^+\nu_\mu}\frac{1-\gamma_5}{2} \end{aligned} \quad (1)$$

In the MSSM these couplings are given by:

$$\begin{aligned} \lambda_{h\mu^+\mu^-} &= -\frac{\sin\alpha}{\cos\beta} \quad , \quad \lambda_{H\mu^+\mu^-} = \frac{\cos\alpha}{\cos\beta} \\ \lambda_{A^0\mu^+\mu^-} &= \tan\beta \quad , \quad \lambda_{H^-\mu^+\nu_\mu} = \tan\beta \end{aligned} \quad (2)$$

One can see from the above formula that the CP–odd A^0 and the charged Higgs bosons coupling to the μ^\pm can be enhanced for large $\tan\beta$.

The momenta of the incoming μ^+ and μ^- , outgoing gauge boson V (W^\pm or Z) and outgoing Higgs scalar S (H^\pm or A^0) are denoted by p_{μ^+} , p_{μ^-} , p_V and p_S , respectively. Neglecting the muon mass m_μ , the momenta in the centre of mass of the $\mu^+\mu^-$ system are given by:

$$\begin{aligned} p_{\mu^-, \mu^+} &= \frac{\sqrt{s}}{2}(1, 0, 0, \pm 1) \\ p_{V, A^0} &= \frac{\sqrt{s}}{2}\left(1 \pm \frac{M_V^2 - M_S^2}{s}, \pm \frac{1}{s}\lambda^{\frac{1}{2}}(s, M_V^2, M_S^2)\sin\theta, 0, \pm \frac{1}{s}\lambda^{\frac{1}{2}}(s, M_V^2, M_S^2)\cos\theta\right), \end{aligned}$$

Here $\lambda(x, y, z) = x^2 + y^2 + z^2 - 2xy - 2xz - 2yz$ is the two body phase space function and θ is the scattering angle between μ^+ and S ; M_V is the mass of the gauge boson V and M_S is the mass of the Higgs scalar S . In the case of H^+H^- production replace V by S . The Mandelstam variables are defined as follows:

$$\begin{aligned} s &= (p_{\mu^-} + p_{\mu^+})^2 = (p_V + p_S)^2 \\ t &= (p_{\mu^-} - p_V)^2 = (p_{\mu^+} - p_S)^2 = \frac{1}{2}(M_V^2 + M_S^2) - \frac{s}{2} + \frac{1}{2}\lambda^{\frac{1}{2}}(s, M_V^2, M_S^2)\cos\theta \\ u &= (p_{\mu^-} - p_S)^2 = (p_{\mu^+} - p_V)^2 = \frac{1}{2}(M_V^2 + M_S^2) - \frac{s}{2} - \frac{1}{2}\lambda^{\frac{1}{2}}(s, M_V^2, M_S^2)\cos\theta \\ s + t + u &= M_V^2 + M_S^2 \end{aligned}$$

2.1 $\mu^+\mu^- \rightarrow H^+H^-$

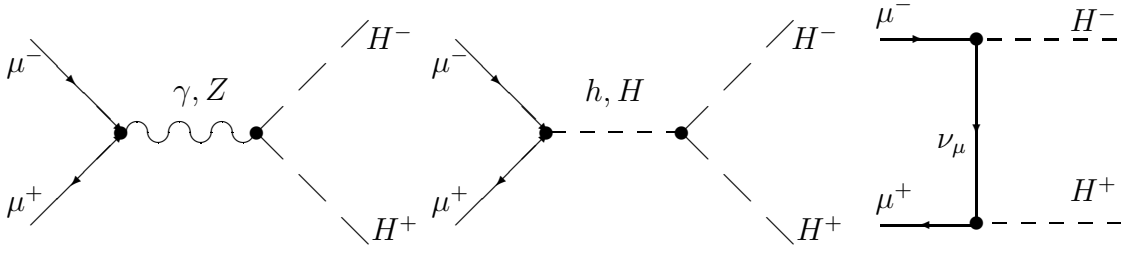


Figure.1

This process proceeds via the conventional Drell–Yan mechanism $\mu^+\mu^- \rightarrow \gamma^*, Z^* \rightarrow H^+H^-$, the analogy of $e^+e^- \rightarrow \gamma^*, Z^* \rightarrow H^+H^-$. Since $m_\mu \approx 200m_e$ one may consider the s–channel and t–channel diagrams (see Fig. 1), whose analogies at e^+e^- colliders would be suppressed by factors of m_e . The s–channel diagrams would be maximised for $\sqrt{s} = M_h$ or M_H , although in the context of the MSSM this condition would not allow on–shell pair production of H^\pm . This can be seen from the fact that $\sqrt{s} \geq 2M_{H^\pm}$ and $\sqrt{s} \approx M_h$ or M_H cannot be simultaneously satisfied in the MSSM. In contrast, such s–channel diagrams were considered in Ref.[14] for squark production via the process $\mu^+\mu^- \rightarrow \tilde{q}\tilde{q}$, and were shown to cause a doubling of the cross–section at resonance. The t–channel diagram in Fig. 1 suffers from Yukawa coupling suppression at two vertices. In the calculation we shall use the following notation:

$$\begin{aligned}
Y_V &= -Y_A = \frac{m_\mu^2}{4s_W^2 M_W^2} \lambda_{H^-\mu\nu\mu}^2 \\
a_h &= -\frac{g_{hH^+H^-} m_\mu \lambda_{h\mu^+\mu^-}}{2M_W s_W}, \quad a_H = -\frac{g_{HH^+H^-} m_\mu \lambda_{H\mu^+\mu^-}}{2M_W s_W} \\
a_1 &= -2\frac{1}{s} - \frac{1}{2s_W^2 c_W^2} \frac{g_H g_V}{s - M_Z^2 + iM_Z \Gamma_Z} - \frac{Y_V}{t} \\
a_2 &= \frac{1}{2s_W^2 c_W^2} \frac{g_H g_A}{s - M_Z^2 + iM_Z \Gamma_Z} - \frac{Y_A}{t} \\
a_3 &= \frac{a_h}{s - M_h^2 + iM_h \Gamma_h} + \frac{a_H}{s - M_H^2 + iM_H \Gamma_H} + \frac{m_\mu Y_V}{t}
\end{aligned} \tag{3}$$

where $g_V = -(1 - 4s_W^2)/2$, $g_A = -1/2$ and $g_H = -c_W^2 + s_W^2$. The coupling $g_{hH^+H^-}$ and $g_{HH^+H^-}$ (normalised to electric charge e) are given by:

$$\begin{aligned}
g_{HH^+H^-} &= -\frac{1}{s_W} \left\{ M_W \cos(\beta - \alpha) - \frac{M_Z}{2c_W} \cos 2\beta \cos(\beta + \alpha) + \epsilon \frac{\cos \alpha \cos^2 \beta}{2c_W M_Z \sin \beta} \right\} \\
g_{hH^+H^-} &= -\frac{1}{s_W} \left\{ M_W \sin(\beta - \alpha) + \frac{M_Z}{2c_W} \cos 2\beta \sin(\beta + \alpha) + \epsilon \frac{\sin \alpha \cos^2 \beta}{2c_W M_Z \sin \beta} \right\}
\end{aligned}$$

Where

$$\epsilon = \frac{3G_F m_t^4}{\sqrt{2}\pi^2 \sin^2 \beta} \log \left[\frac{m_{\tilde{t}_1} m_{\tilde{t}_2}}{m_t^2} \right] \tag{4}$$

The ϵ term corresponds to the leading log 1-loop corrections [15] to the trilinear couplings. We will include also these leading log corrections to the Higgs-masses and to the mixing angles.

The square amplitude is given by:

$$|M|^2 = e^4 \left\{ (|a_1|^2 + |a_2|^2) \frac{s^2}{2} \beta_H^2 \sin^2 \theta - 2|a_2|^2 m_\mu^2 s \beta_H^2 + 2|a_3|^2 s + 4\Re(a_1 a_3) m_\mu s \beta_H \cos \theta \right\} \quad (5)$$

with $\beta_H^2 = 1 - 4M_{H^\pm}^2/s$. The differential cross-section is given by:

$$\frac{d\sigma}{d\Omega} = \frac{\beta_H}{64\pi^2 s} \frac{1}{4} |M|^2 \quad (6)$$

2.2 $\mu^+ \mu^- \rightarrow H^\pm W^\mp$

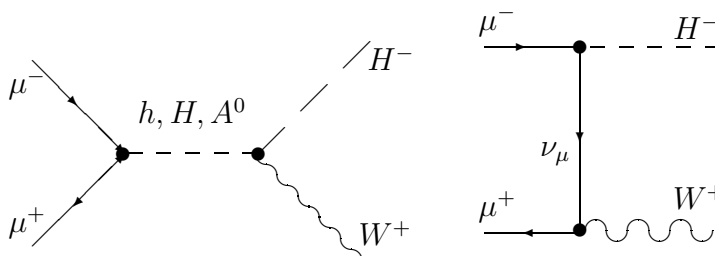


Figure.2

Single H^\pm production may proceed via an s-channel resonance mediated by h^0 , H^0 or A^0 , and by t-channel exchange of ν_μ (see Fig. 2). All are negligible at an e^+e^- collider due to the smallness of m_e . The loop induced contributions to $e^+e^- \rightarrow H^\pm W^\mp$ were considered in Ref.[16] and shown to reach a few fb at very low values of $\tan \beta$, a region disfavoured in the MSSM. Potential advantages of $\mu^+ \mu^- \rightarrow H^\pm W^\mp$ over standard pair production are the following:

- $\mu^+ \mu^- \rightarrow H^\pm W^\mp$ is sensitive to the $H^\pm \mu^\mp \nu_\mu$ Yukawa coupling, which is model dependent, and hence provides information on the underlying Higgs structure. For example, we shall see that a 2HDM with the Model I type structure would not register a signal in this channel. In contrast $\mu^+ \mu^- \rightarrow \gamma^*, Z^* \rightarrow H^+ H^-$ has a model independent rate.
- Single H^\pm production is less phase space suppressed than H^\pm pair production, and would also allow greater kinematical reach at a given collider (on-shell production up to $\sim \sqrt{s} - M_W$).
- The t-channel contribution may be sizeable and does not require $\sqrt{s} \approx M_{res}$ to be significant, where M_{res} is the mass of a neutral Higgs s-channel resonance. This is in contrast to other novel production processes at $\mu^+ \mu^-$ colliders, which usually require the condition $\sqrt{s} \approx M_{res}$.

The differential cross-section for $\sigma(\mu^+\mu^- \rightarrow H^\pm W^\mp)$ may be written as follows:

$$\frac{d\sigma}{d\Omega} = \frac{\lambda^{\frac{1}{2}}(s, M_{H^\pm}^2, M_W^2)}{64\pi^2 s^2} |\mathcal{M}|^2 \quad (7)$$

The matrix element squared is given by:

$$\begin{aligned} |\mathcal{M}|^2 = & \frac{sg^4 m_\mu^2}{32M_W^4} [(|a_V|^2 + |a_A|^2) \lambda(s, M_{H^\pm}^2, M_W^2) + 2a_t^2 (2M_W^2 p_T^2 + t^2) \\ & + 2a_t (M_{H^\pm}^2 M_W^2 - sp_T^2 - t^2) \Re(a_V - a_A)] \end{aligned} \quad (8)$$

Where $p_T^2 = \lambda(s, M_{H^\pm}^2, M_W^2) \sin^2 \theta / 4s$ and the couplings a_V, a_A and a_t are given by:

$$a_V = \left(\frac{\cos(\alpha - \beta) \lambda_{h\mu^+\mu^-}}{s - M_h^2 + iM_h \Gamma_h} + \frac{\sin(\alpha - \beta) \lambda_{H\mu^+\mu^-}}{s - M_H^2 + iM_H \Gamma_H} \right) \quad (9)$$

$$a_A = \frac{\lambda_{A\mu^+\mu^-}}{s - M_A^2 + iM_A \Gamma_A} \quad (10)$$

$$a_t = \frac{\lambda_{H^-\mu^+\nu_\mu}}{t} \quad (11)$$

The mixing angle dependence of the Higgs–Fermion–Fermion couplings is contained in $\lambda_{h\mu^+\mu^-}$, $\lambda_{H\mu^+\mu^-}$, $\lambda_{A\mu^+\mu^-}$ and $\lambda_{H^-\mu^+\nu_\mu}$.

Our formula agrees with that for $b\bar{b} \rightarrow H^\pm W^\mp$ in Ref. [10], with the replacements $m_t \rightarrow m_{\nu_\mu}$ and $m_b \rightarrow m_\mu$. Due to CP-invariance the rate for W^+H^- and W^-H^+ production is identical. The total cross section takes the following form:

$$\begin{aligned} \sigma(\mu^+\mu^- \rightarrow W^+H^-) = & \frac{G_F m_\mu^2}{16\pi s^2} \{ (|a_V|^2 + |a_A|^2) \lambda(s, M_{H^\pm}^2, M_W^2) s \\ & + 2 \tan \beta [\Re(a_A - a_V) (M_{H^\pm}^2 + M_W^2 - s) s + (s - 4M_W^2) \tan \beta] \lambda^{\frac{1}{2}}(s, M_{H^\pm}^2, M_W^2) \\ & - 4M_W^2 \tan \beta [\Re(a_V - a_A) M_{H^\pm}^2 s + (M_{H^\pm}^2 + M_W^2 - s) \tan \beta] F(s, M_{H^\pm}^2, M_W^2) \} \end{aligned} \quad (12)$$

with:

$$F(s, M_S^2, M_V^2) = \text{Log} \left[\frac{M_S^2 + M_V^2 - s - \lambda^{\frac{1}{2}}(s, M_S^2, M_V^2)}{M_S^2 + M_V^2 - s + \lambda^{\frac{1}{2}}(s, M_S^2, M_V^2)} \right]$$

2.3 $\mu^+\mu^- \rightarrow A^0 Z$

As depicted in Fig. 3, this process proceeds in a very similar way to that for $\mu^+\mu^- \rightarrow H^\pm W^\mp$, except there are two t-channel diagrams. The process $\mu^+\mu^- \rightarrow Z\phi^0$, where ϕ^0 is the SM Higgs boson, has been considered in Ref. [17]. Our calculation differs since there is no s-channel Z exchange for $\mu^+\mu^- \rightarrow A^0 Z$ in the MSSM. Instead there are two s-channel Higgs exchange diagrams of similar magnitude to the t-channel diagram, giving rise to strong interference. In addition $\tan \beta$ plays an important role. In the SM the s-channel Z exchange is the dominant diagram at the collider energy we consider ($\sqrt{s} = 500$ GeV), and so interference is minimal.

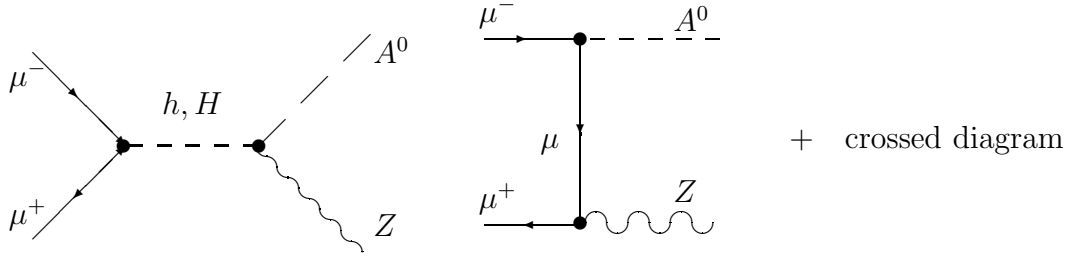


Figure.3

The mechanism $\mu^+\mu^- \rightarrow A^0Z$ would provide an alternative way of searching for A^0 whose detection is not guaranteed at the LHC or a $\sqrt{s} = 500$ GeV e^+e^- collider. At the latter this is because the conventional production mechanism $e^+e^- \rightarrow Z^* \rightarrow A^0H^0$ would be closed kinematically for $M_A \approx M_H \geq 250$ GeV, and $e^+e^- \rightarrow Z^* \rightarrow A^0h^0$ ($\sim \cos^2(\beta - \alpha)$) is strongly suppressed for $M_A \geq 200$ GeV. The proposed search at a $\mu^+\mu^-$ collider for $M_A \geq \sqrt{s}/2$ is by doing a scan over \sqrt{s} energies, in order to find a resonance at $\sqrt{s} = M_A$, or by running the collider at full \sqrt{s} and looking for peaks in the $b\bar{b}$ mass distribution (Bremsstrahlung tail method). These methods are competitive and both may allow detection up to $M_A \approx \sqrt{s}$ as long as $\tan\beta \geq 4 - 6$. However, both may provide quite a demanding challenge for detector resolution and machine design (see Ref. [8]), and it is too early to say with certainty if they would be feasible methods in practice. With this in mind we consider the process $\mu^+\mu^- \rightarrow A^0Z$. With a sizeable rate for $\sigma(\mu^+\mu^- \rightarrow AZ)$, A^0 could be discovered first in this channel, and then the beams could be adjusted to $\sqrt{s} = M_A$ for precision studies. In addition, $\mu^+\mu^- \rightarrow A^0Z$ probes greater masses of M_A than $e^+e^- \rightarrow Z^* \rightarrow A^0H^0$, and becomes another option to first discover A^0 (if discovery has been elusive at the LHC or a $\sqrt{s} = 500$ GeV e^+e^- collider). The matrix element squared may be written as:

$$\begin{aligned}
|\mathcal{M}|^2 &= \frac{sg^4m_\mu^2}{32M_W^4} [|a_V|^2 \lambda(s, M_A^2, M_Z^2) - 2a_{t1}g_A(M_A^2M_Z^2 - sp_T^2 - t^2)\Re(a_V) \\
&\quad - 2a_{t2}g_A(M_A^2M_Z^2 - sp_T^2 - u^2)\Re(a_V) \\
&\quad + (g_A^2 + g_V^2) \{ a_{t1}^2(2M_Z^2p_T^2 + t^2) + a_{t2}^2(2M_Z^2p_T^2 + u^2) \} \\
&\quad - 2(g_A^2 - g_V^2)a_{t1}a_{t2}(2M_Z^2p_T^2 + 2M_A^2M_Z^2 - tu)] \quad (13)
\end{aligned}$$

with a_V the same as in Section 2.2 and

$$a_{t1} = \frac{\lambda_{A\mu^+\mu^-}}{t - m_\mu^2}, \quad a_{t2} = \frac{\lambda_{A\mu^+\mu^-}}{u - m_\mu^2} \quad (14)$$

The differential cross-section follows from eq(7) with the changes $M_{H^\pm} \rightarrow M_A$ and $M_W \rightarrow M_Z$.

The total cross-section is given by:

$$\begin{aligned}
\sigma(\mu^+\mu^- \rightarrow A^0 Z) &= \frac{G_F m_\mu^2}{32\pi s^2} \{ [4s(g_A^2 - g_V^2) \tan^2 \beta + 2s|a_V|^2 \lambda(s, M_A^2, M_Z^2)] \lambda^{\frac{1}{2}}(s, M_A^2, M_Z^2) \\
&+ [8s\Re(a_V)g_A(M_A^2 + M_Z^2 - s) \tan \beta - 8(g_A^2 - g_V^2)M_Z^2 \tan^2 \beta \\
&+ 4(g_A^2 + g_V^2)(s - 4M_Z^2) \tan^2 \beta] \lambda^{\frac{1}{2}}(s, M_A^2, M_Z^2) \\
&+ \frac{F(s, M_A^2, M_Z^2)}{(M_A^2 + M_Z^2 - s)} [-8M_Z^2 \tan \beta (-2\Re(a_V)g_A M_A^2 (M_A^2 + M_Z^2 - s)s \\
&+ (2(g_A^2 - g_V^2)M_A^2(M_Z^2 - s) + (g_A^2 + g_V^2)(M_A^2 + M_Z^2 - s)^2) \tan \beta) \} \} \quad (15)
\end{aligned}$$

3 Numerical results

We now present our numerical analysis in the context of the MSSM. We take $\sqrt{s} = 500$ GeV and assume integrated luminosities of the order 50 fb^{-1} .

In Fig. 4 we plot $\sigma(\mu^+\mu^- \rightarrow H^\pm W^\mp)$, defined as the sum of H^+W^- and H^-W^+ production, as a function of M_{H^\pm} , varying $\tan\beta$ from 20 to 50. We also include the tree-level rate for $\sigma(e^+e^- \rightarrow H^+H^-)$ in order to show the advantage of a $\mu^+\mu^-$ collider over an e^+e^- collider. One can see that the single production mode gains in importance with increasing $\tan\beta$, and offers detection possibilities for M_{H^\pm} up to $\sqrt{s} - M_W$. This compares favourably with the reach at an e^+e^- collider.

The slight dip and rise of the curves arises due to the H^0 and A^0 mediated s -channel contributions increasing in magnitude with M_{H^\pm} , which compensates for the phase space suppression until the kinematical limit is approached. This can be seen from the fact that since $M_{H^\pm} \approx M_H \approx M_A$, larger M_{H^\pm} causes both M_H and M_A to be closer to \sqrt{s} (i.e. the resonance condition).

It is clear from the graphs that for $\tan\beta \geq 20$ one has $\sigma(\mu^+\mu^- \rightarrow H^\pm W^\mp) \geq 5$ fb, which would give a sizeable number of singly produced H^\pm for luminosities of 50 fb^{-1} . One would expect $H^\pm \rightarrow tb$ decays for the mass region of interest and so the main background would be from $t\bar{t}$ production. Such a background [11] was shown to overwhelm the channel $pp \rightarrow H^\pm W^\mp$ [10] at the LHC. However, at a $\sqrt{s} = 500$ GeV muon collider $\sigma(\mu^+\mu^- \rightarrow t\bar{t}) \sim 0.7$ pb in contrast to ~ 800 pb at the LHC. Hence we would expect much better prospects for detection at a muon collider although a full signal-background analysis is beyond the scope of this paper. Previous studies of backgrounds to $H^\pm W^\mp$ production at e^+e^- colliders have been carried out in the context of Higgs triplet models [18], assuming $H^\pm \rightarrow W^\pm Z$ as the main decay channel. Such studies cannot be applied to the MSSM where $H^\pm \rightarrow tb$ decays would dominate.

We note that a 2HDM with the Model I type structure would not register an observable signal in this channel. This is due to the rate being proportional to $\cot^2 \beta$, and so unacceptably small values of $\tan\beta$ would be required in order to allow observable cross-sections.

The process $\mu^+\mu^- \rightarrow A^0 Z$ suffers from smaller cross-sections and these are plotted as a function of M_A in Fig. 5. Given that $\mu^+\mu^- \rightarrow A^0 H^0$ probes M_A up to $\approx \sqrt{s}/2$ the

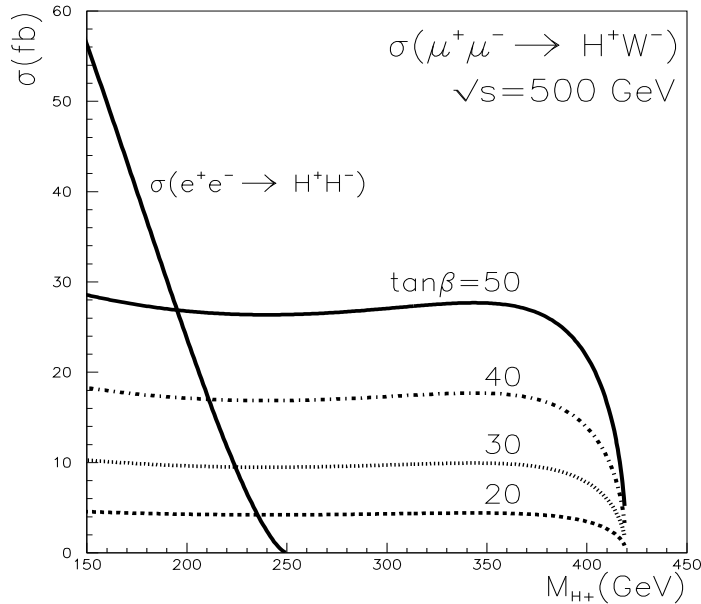


Figure 4: $\sigma(\mu^+\mu^- \rightarrow H^\pm W^\mp)$ as a function of M_{H^\pm} for various values of $\tan\beta$. Also indicated is $\sigma(e^+e^- \rightarrow H^+H^-)$ for the same \sqrt{s} .

region $M_A \geq 250$ GeV is of interest. We see that cross-sections ≥ 1 fb are only attainable in this region for $\tan\beta \geq 30$ and so detection would be restricted to large values of $\tan\beta$. The smallness of the cross-sections is caused by large destructive interference between the s and t channels.

Finally, we consider $\mu^+\mu^- \rightarrow H^+H^-$. We find very small deviations from the rate for $e^+e^- \rightarrow H^+H^-$, of the order a few percent for large values of $\tan\beta$. This can be traced to the fact that the s -channel Higgs exchange diagrams are far from resonance, and the t -channel diagrams are doubly Yukawa suppressed. Since the 1-loop corrections [6] may be much larger than these deviations we do not plot a graph.

4 Conclusions

We have considered the processes $\mu^+\mu^- \rightarrow H^\pm W^\mp$ and $\mu^+\mu^- \rightarrow A^0 Z$ of the MSSM in the context of a high-energy $\mu^+\mu^-$ collider ($\sqrt{s} = 500$ GeV). We showed that $\mu^+\mu^- \rightarrow H^\pm W^\mp$ production offers an attractive new way of searching for H^\pm at such colliders. The cross-section grows with increasing $\tan\beta$ with values as large as 30 fb being attainable for $\tan\beta \geq 50$. With an integrated luminosity of 50 fb^{-1} a significant number of H^\pm could be produced singly up to $M_{H^\pm} \approx \sqrt{s} - M_W$. This compares favourably with the reach

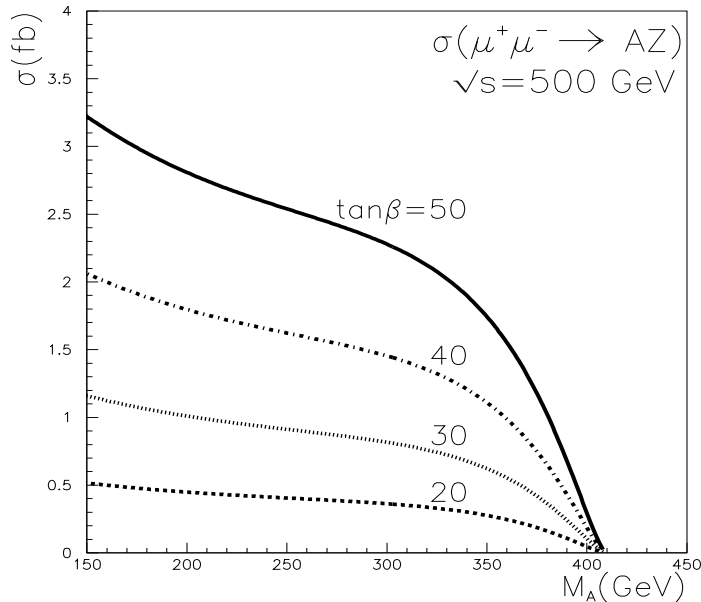


Figure 5: $\sigma(\mu^+\mu^- \rightarrow A^0Z)$ as a function of M_A for various values of $\tan\beta$.

at an e^+e^- collider, which may only probe up to $M_{H^\pm} \approx \sqrt{s}/2$. The main background (assuming $H^\pm \rightarrow tb$ decays) would be from $t\bar{t}$ production, which has a cross-section of 700 fb, 3 orders of magnitude less than at the LHC. We conclude that the mechanism $\mu^+\mu^- \rightarrow H^\pm W^\mp$ represents a novel and attractive way of producing H^\pm at a $\mu^+\mu^-$ collider, and in our opinion merits a detailed signal-background analysis.

Pseudoscalar Higgs production via $\mu^+\mu^- \rightarrow A^0Z$ offers smaller cross-sections, with values of 2 fb or more only possible for large (≥ 40) $\tan\beta$. Charged Higgs pair production has essentially the same rate as that at an e^+e^- collider, with differences of the order of a few percent for large values of $\tan\beta$.

Acknowledgements

A.G. Akeroyd was supported by the Japan Society for Promotion of Science (JSPS). We thank A. Turcot for useful comments.

References

- [1] J.F. Gunion, H.E. Haber, G.L. Kane and S. Dawson, *The Higgs Hunter's Guide* (Addison-Wesley, Reading, 1990).

- [2] S. Komamiya, Phys. Rev. **D38** (1988) 2158; A. Sopczak, Z.Phys. **C65** (1995) 449; S. Moretti and K. Odagiri, J. Phys. **G23** (1997) 537.
- [3] E. Eichten, I. Hinchliffe, K. Lane and C. Quigg, Rev. Mod. Phys. **56** (1984) 579; J. Gunion, H.E. Haber, F.E. Paige, W.K. Tung and S.S.D. Willenbrock, Nucl. Phys. **B294** (1987) 621; R.M. Barnett, H.E. Haber and D.E. Soper, **B306** (1988) 697; D.A. Dicus, J.L. Hewett, C. Kao, and T.G. Rizzo, Phys. Rev. **D40** (1989) 787; V. Barger, R.J.N. Philips and D.P. Roy, Phys. Lett. **B324** (1994) 236; J.L. Diaz-Cruz and O.A. Sampayo, Phys. Rev. **D50** (1994) 6828.
- [4] Jiang Yi, Ma Wen-Gan, Han Liang, Han Meng and Yu Zeng-hui; J. Phys. **G24** (1998) 83; J. Phys. **G23** (1997)385; A. Krause, T. Plehn, M. Spira and P.W. Zerwas, Nucl. Phys. **B519** (1998) 85; S. Moretti and K. Odagiri, Phys. Rev. **D55** (1997) 5627; Li Gang Jin, Chong Sheng Li, R.J. Oakes and Shou Hua Zhu, hep-ph/9907482; A.A. Barrientos Bendezu and B.A. Kniehl, hep-ph/9908385; O. Brein and W. Hollik, hep-ph/9908529.
- [5] K. Odagiri. Phys. Lett. **B452** (1999) 327; K. Odagiri, hep-ph/9901432; D.P. Roy, Phys. Lett. **B459** (1999) 607; D.J. Miller, S. Moretti, D.P. Roy and W.J. Stirling, hep-ph/9906230; M. Drees, M. Guchait and D.P. Roy, hep-ph/9909266, S. Moretti and D.P. Roy, hep-ph/9909435.
- [6] A. Arhrib, M. Capdequi Peyranère and G. Moultaka, Phys. Lett. **B341** (1995) 313; M.A. Diaz and Tonnis A. ter Veldhuis, hep-ph/9501315; A. Arhrib and G. Moultaka, hep-ph/9808317, to appear in Nucl. Phys. B.
- [7] Combined Experimental Limits; ALEPH 99-081 CONF 99-052; DELPHI 99-142 CONF 327; L3 Note 2442; OPAL Technical Note TN-614.
- [8] *Proceedings of the Workshop on Physics at the First Muon Collider and front end of a Muon Collider*, Fermilab, November 6-9, 1997; $\mu^+\mu^-$ Collider: a Feasibility Study, BNL-52503, Fermilab-Conf-96/092, LBNL-38946, July 1996; Phys. Rep. 286 (1996) 1.
- [9] J. Gunion, hep-ph/9802258, V. Barger, hep-ph/9803480.
- [10] A.A. Barrientos Bendezu and B.A. Kniehl, Phys. Rev. **D59** (1999) 015009.
- [11] S. Moretti and K. Odagiri, Phys. Rev. **D59** (1999) 055008.
- [12] A.G. Akeroyd, A. Arhrib and M. Capdequi Peyranère, Mod. Phys. Lett. **A14** (1999) 2093.
- [13] A. Djouadi, V. Driesen, W. Hollik and A. Kraft, Eur. Phys. J. **C1** (1998) 163.
- [14] A. Bartl, H. Eberl, K. Hidaka, S. Kraml, W. Majerotto, W. Porod and Y. Yamada, Phys. Rev. **D58** (1999) 115002.

- [15] Y. Okada, M. Yamaguchi and T. Yanagida, *Prog. Theo. Phys.* **85** (1991) 1; H. Haber and R. Hemping, *Phys. Rev. Lett.* **66** (1991) 1815; J. Ellis, G. Ridolfi and F. Zwirner, *Phys. Lett.* **B257** (1991) 83; R. Barbieri, F. Caravaglios and M. Frigeni, *Phys. Lett.* **B258** (1991) 167.
- [16] Shou Hua Zhou, hep-ph/9901221.
- [17] V.A. Litvin and F.F. Tikhonin, hep-ph/9704417; F.F. Tikhonin, IFVE-98-18; V.A. Litvin and F.F. Tikhonin, IFVE-98-19.
- [18] K. Cheung, R.J.N. Phillips and A. Pilaftsis, *Phys. Rev.* **D51** (1995) 4731; D.K. Ghosh, R.M. Godbole and B. Mukhopadhyaya, *Phys. Rev.* **D55** (1997) 3150.